Environmental Effects on the Local Density of States of CdSe Quantum Dots on a Au Substrate

P. R. Stollenwerk*[1], M. Olson Hummon[2], A. J. Stollenwerk[2], M. Kemei[3] and V. Narayanamurti[2]

[1] Department of Physics, The Ohio State University
[2] School of Engineering and Applied Sciences, Harvard University
[3] Scanning Probe Microscopy Institute, Mount Holyoke College

Scanning tunneling microscopy was used to image sub-monolayer CdSe (d = 10 nm) quantum dots (QDs) on a gold substrate. After imaging the surface, scanning tunneling spectroscopy was performed on a single QD in the middle of a cluster, at the edge of a cluster and completely isolated from other QDs. Data showed that the zero-conductance region decreased with respect to the number of neighboring dots. A classical electrostatic screening model was used to analyze this effect.

Introduction

Quantum dots (QDs) are small clusters of atoms that form an essentially zero-dimensional structure. These clusters of atoms range in size from approximately 2 to 10 nm in diameter. The electrical and optical properties of QDs vary from their bulk counterparts due to quantum confinement effects. The applications of quantum dots include light emitting diodes (LEDs) and solar cells.[3, 8] Studying the properties of QDs allows for a better fundamental understanding of these structures and can potentially lead to more efficient devices.

In the past, electro and photo-luminescence has been used to study the optical bandgaps of these structures as a function of size and material composition.[7] These techniques give average QD properties over a large surface area. Though this information gives much insight into QDs, it is desirable to have the ability to investigate individual QDs. Due to its sub-nanometer resolution, scanning tunneling microscopy (STM) has proven successful at investigating individual QDs.[1,10] In STM, a sharp metallic tip is brought within a few angstroms of a conductive surface. When a bias is applied between the tip and a sample, electrons can tunnel due to a significant overlapping of their wave functions. Combining STM with scanning tunneling spectroscopy (STS), one can obtain the local density of states (LDOS) on a single QD. In this paper STM and STS were used to investigate how the local environment affected the electronic structure. This was accomplished by measuring the LDOS of a single QD that was in the middle of a cluster, at the edge of a cluster and completely isolated from other QDs. This data showed that the local environment did in fact have an influence on the LDOS.

Background

Metals and Semiconductors

Solids have three different types of structures: amorphous, crystalline or poly-

About the Author

Patrick Stollenwerk is currently a junior at The Ohio State University double majoring in physics and mathematics. He plans to attend graduate school in physics. At the moment, he is working in Dr. Lemberger's research group. His research consists of writing a computer program that models thin superconducting films.

(Patrick's manuscript was the first research article submitted to *JUROS*)

crystalline. An amorphous solid consists of atoms that are arranged in a random fashion. A crystalline solid consists of atoms with a periodic ordered structure spanning all three dimensions, while a polycrystalline solid is composed of a random array of many smaller crystals in different orientations. All of these types of solids exhibit metallic and semiconducting properties, but the crystal lattice is the easiest to understand. For this reason, this section will be limited to this case.

A crystal lattice consists of periodically spaced atoms. The spacing of these atoms is such that the electron wave functions of these atoms overlap with each other. This causes electron waves to interfere either constructively or destructively depending on the energy of the electron. In the areas where constructive interference occurs, available states exist for the electrons to occupy. An energy range in which these states are available is known as an energy band. Conversely, where destructive interference occurs, an energy bandgap is present.

The energy band is only partially filled in a metal, giving room for electrons to move around, allowing a metal to be conductive. An energy band is entirely filled in a semiconductor. It is difficult for the electrons to move around, making semiconductors poor conductors. In order for a semiconductor to be conductive the semiconductor must be given enough energy for the electron to surmount the bandgap and occupy the next available energy band. Raising the temperature of the semiconductor is one way to do this. The highest filled band in a semiconductor is known as the valence band (Ev) and the next available energy band is known as the conduction band (Ec). The difference between the valence band and the conduction band is the bandgap (Eg). The Fermi level (Ef) is defined as the highest occupied energy level. In a metal, the Fermi level lies inside an energy band (Figure 1a). In a semiconductor it lies within an energy bandgap (Figure 1b).

Quantum Dots

Unlike bulk semiconductors and metals, electrons in QDs are confined in three spatial dimensions that are similar in size to the wavelength of these electrons. Due to this, they have properties that are similar to bulk solids as well as those of isolated atoms. These properties are surprisingly well approximated by the "particle in a box" problem in quantum mechanics.

STM

In STM the tip must be within tunneling range of the sample. In order to establish the tunneling range, a bias of
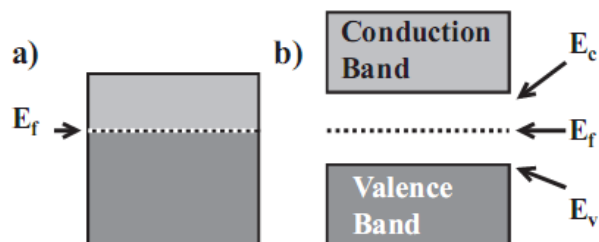

Figure 1. (a) Energy band diagram of metal and (b) energy band diagram of a semiconductor.

several volts between the tip and sample is applied. The STM then follows a pattern of movements to bring the tip into tunneling distance from the sample. This is done using a combination of fine and coarse motors. The fine motor expands throughout its entire range, bringing the tip closer to the surface. The STM searches for a tunneling current as the tip is brought closer to the surface. If no current is found the fine motor fully retracts and the coarse motor brings the tip to a distance equal to half the full extension range of the fine motor. This cycle will repeat until a tunneling current is found. Once the coarse positioner has brought the tip into tunneling range, the feedback loop is put into effect. The feedback loop reacts to any changes in the tunneling current and adjusts the height as necessary to bring the current back to the set point. A current set point is chosen for the feedback loop to maintain. The tip is then rastered back and forth in successive parallel lines. As this occurs, the feedback loop maintains the set point by constantly adjusting the tip-to-tip sample distance. The STM software then records the displacement of the tip, giving a relative height. By combining all the successive scans, a topographical map of the surface can be visualized.

STM can also perform scanning tunneling spectroscopy (STS). STS is accomplished by pausing the scan, choosing a tip location and disabling the feedback loop. Once the feedback loop is disabled, the fine motor can be adjusted to choose a starting height and corresponding tunneling current. When the spectroscopy is initiated, the tip holds its position and height and then sweeps the bias voltage through a chosen range. As the voltage sweep occurs, the tunneling current is mapped as a function of voltage.

The software will also record differential current values (dI/dV) which provide information about the LDOS. When a bias is applied to the tip, the Fermi level of the tip changes relative to the Fermi level of the sample. In the case of a semiconductor, when a negative bias is applied to the tip, tunneling will not occur if the applied bias is not as high as the conduction band (Figure 2a). When the bias on the tip is sufficiently negative, electrons in the tip will be able to tunnel into the conduction band of a semiconductor (Figure

SCIENCES

2b). Similarly, if the bias on the tip is not positive enough, tunneling will not occur, because the Fermi level of the tip is greater than the valence band of the sample (Figure 2c). If the bias on the tip is sufficiently positive, electrons from the valence band will be able to tunnel from the sample to the tip (Figure 2d). If no bias is applied, then no tunneling will occur.

Experimental Procedures

Quantum Dot Synthesis and Sample Production

Samples were prepared by the Bulovic group at MIT and the dots were grown by the Bawendi group using what is typically referred to as the "hot injection method."[6] This process involved the injection of two precursors into a hot, $\sim 300^\circ$ C, solvent. For the subject CdSe dots, an organometallic containing cadmium [(CH3)2Cd] and trioctylphosphine selenide (TOPSe) was used as the precursors. Once added to the solvent, a supersaturated solution was formed and homogenous crystal growth began almost instantly. The solution was brought back down to room temperature to prevent any further crystal growth. From this point, a much more controlled growth was maintained by varying the temperature. Left on their own, the nanocrystals would naturally aggregate and precipitate. Ligands were attached to the surface of the dots that kept them dissolved in solution by counteracting their natural tendency to aggregate. To purify and isolate dots of different sizes, methanol was added to the solution. Since the largest crystals also had the largest kinetic energies and methanol lowered the energy necessary to precipitate, the largest dots in the solution would aggregate. This allowed for a subset with a smaller range of sizes to be selected and separated by centrifugation from a set that already had a relatively narrow range. The selected batch was re-dissolved in a solution of chloroform and the average dot size was determined using optical absorption spectroscopy. With the proper dot size achieved, the solution was spuncoat onto a flexible polymer and then stamped onto a gold (Au) substrate.

Tip Fabrication

Tungsten (W) tips used for scanning and spectroscopy were made in house through electrochemical etching. A straightened tungsten wire was fed through the center of a Au wire loop with a diameter of about 1 cm. A film of 5 M potassium hydroxide (KOH) was then placed across the loop. An AC voltage (5 V) was applied to the circuit, and oxidized W on the surface and in the wire was etched away. As the tungsten was etched away, gravity continu-
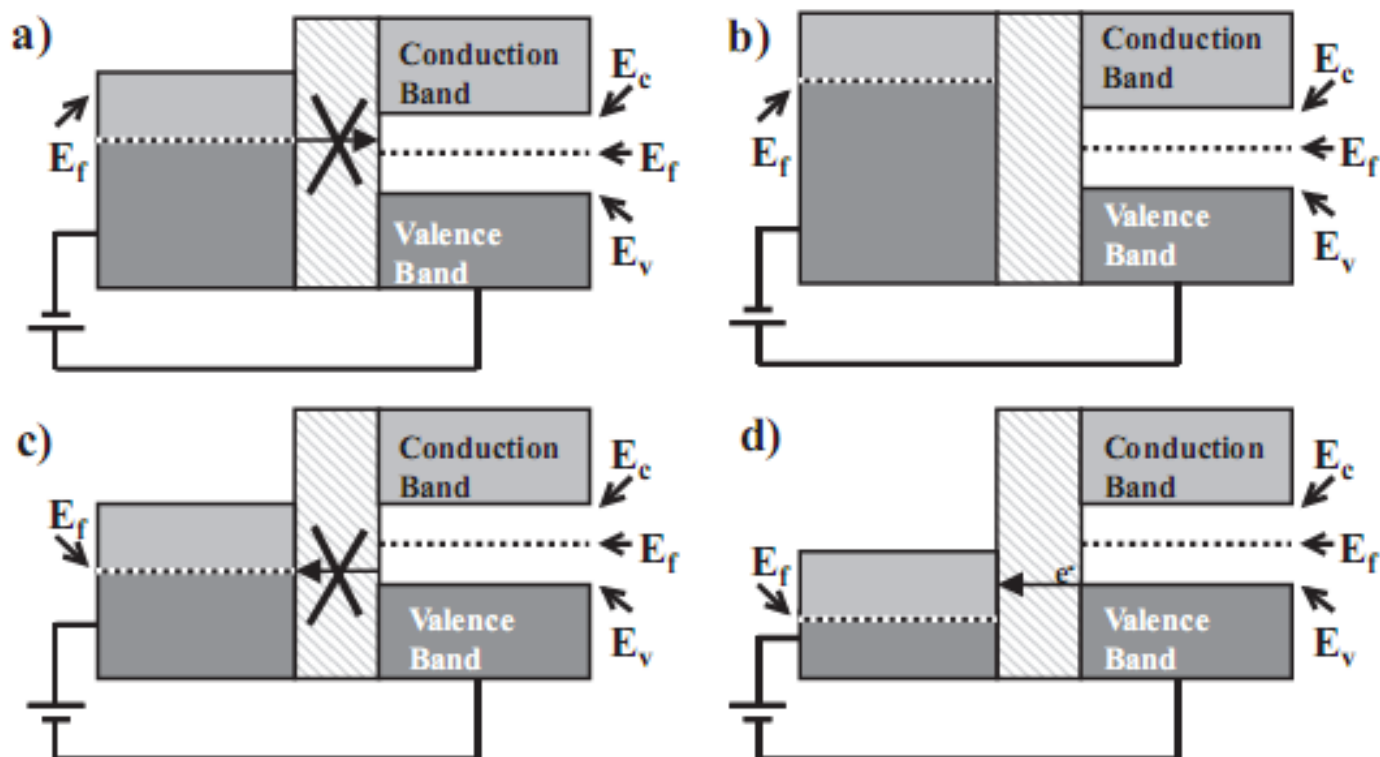

Figure 2. (a) Positive tip bias - cannot tunnel into bandgap. (b) Increased positive tip bias - tunneling occurs from tip into conduction band. (c) Negative tip bias - cannot tunnel into bandgap. (d) Increased negative tip bias - tunneling occurs from valence band into tip.

ously stretched the thinning wire until it snapped, creating a very sharp tip. The tip was caught in a container of shaving cream with the sharp end sticking out. The tip was rinsed and then observed under an optical microscope to detect any irregular shapes that were a sign of instability. Once no irregularities were observed (Figure 3), the tip was ready to be mounted and placed in the STM.

Mounting the tip into the magnetic tip holder was a very tedious task and required much care. To prepare the holder for tip mounting, a small piece (~ 5 mm) of hypodermic stainless steel tubing was cut, and one end was opened wide enough for the tip to fit. The tube was forced into the holder using a bench vise. The length of holder was checked to decide how much of the tip should protrude from the end before inserting the tip. With a sufficient amount exposed, the tip was set inside the tubing with a pair of tweezers. The tube was then crimped by a wire cutter, such that the tip was fastened and ohmic contact was secured.

The STM at Rowland Institute at Harvard

The STM was located in an electrically insulated room to reduce any external noise. It was left at room temperature (~ 300 K) and all scanning occurred under high vacuum (~ 10E-8 Torr). A turbo pump was used to initially evacuate the chambers and an ion pump was used to lower and maintain the pressure. Ion pumps were used because they did not have moving parts that could cause vibrations. The system was composed of a STM chamber, a load lock and a transfer chamber. Each chamber was connected by magnetic transfer drives and could be isolated by gate valves. The STM was held aloft by air-legs that dampened low-frequency noise. The tip and sample were located on a floating platform inside the chamber held up by springs to suppress high-frequency noise. To further isolate the system from vibrations, copper fins around the floating platform were surrounded by magnets that formed an eddy dampening system to oppose any motion.

Due to the design of the transferring process, a tip had to be put into the STM chamber before the sample. A tip was placed onto a mount by magnetically attaching it to a fork hanging off the center of the mount. The mount was screwed onto the end of the magnetic drive in the load lock. The turbo pump then evacuated the load lock. Once the turbo pump had reached 56,000 rpm, the valve between the load lock and the transfer chamber was opened and the tip was inserted into the transfer chamber. Next, the valve was closed and the gate separating the transfer chamber from the STM chamber was opened. The tip was picked up by another magnetic drive and placed into the STM chamber. It was carefully brought in until the piezo-motors were within reach. On the end of the piezo-motor was a magnet inside a ceramic cup that allowed it to attract and support the tip holder. Using a camera to view the progress, the course positioners were adjusted in the X, Y and Z direc-
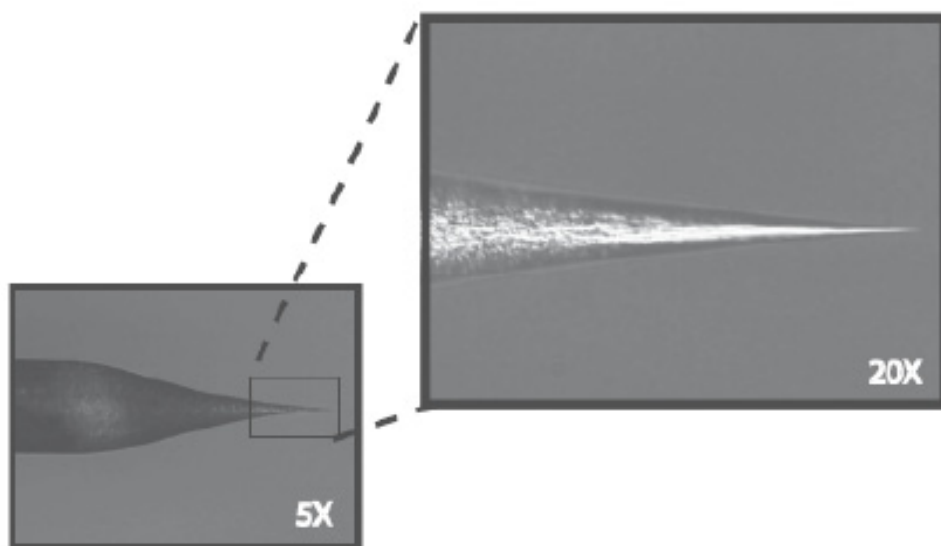
Figure 3. A picture of a tip used in the STM. Note the smooth and stable shape forming a sharp tip.
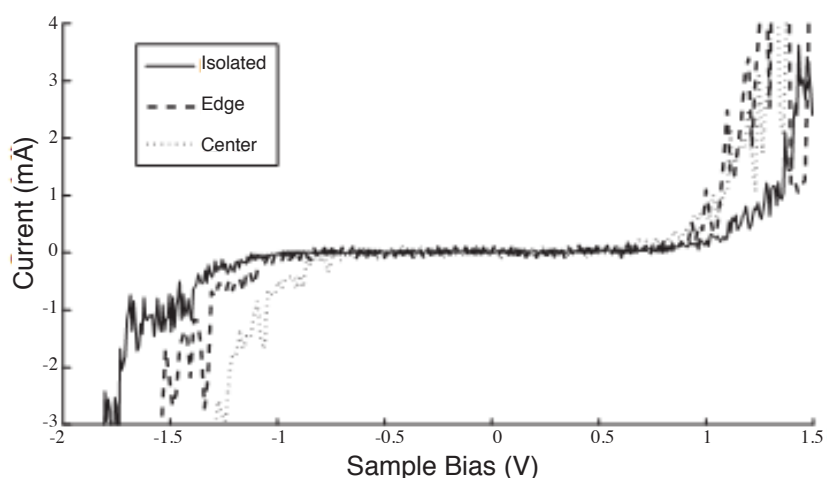

Figure 4. I-V curves for isolated dots, edge of cluster dots and center of cluster dots. The voltage range of zero-conductance corresponds to the apparent bandgap.

tions in order to attach to the tip holder and remove it from the fork. Lastly, the magnetic drive was retracted and the gate closed.

Any sample placed in the STM had to follow a strict procedure to limit contamination and also to prevent damage to the microscope. In a clean hood, the sample was placed on top of a thin Si layer and the two were clamped onto a copper mount while taking care to avoid any scratching or touching of the surface. A multi-meter was used to measure the resistivity across the sample. A low resistivity (~ 1 Ω) ensured that the sample had been properly clamped. The sample mount was screwed onto the end of the magnetic drive in the load lock after the resistivity was verified. The same steps were repeated with the tip until the sample reached the STM chamber. The sample was then placed in the microscope until locked in position. This time the magnetic drive was unscrewed from the sample before it was retracted and the gate was closed.

With the tip and sample in place, the STM could be prepared for scanning. Resistivity of the sample was again checked to verify a sample bias could be established. The STM chamber was inspected in order to confirm that the

springs were free and the platform was properly floating. The air-legs were also checked and the turbo pump shut down. At this point the tip was ready for a manual approach.

In order to allow for a manual approach, a camera was focused on the tip. The course positioners were used to bring the tip within a few hundred microns from the surface. The lights were turned off and the door to the STM room was closed once the tip approached a safe distance from the surface.

Before the computer took over to bring the tip into tunneling range (as previously described) the bias was set to > 6 V, the set point to 4 nA, the gain to > 6, the time constant to < 2 and the fine positioner controls to 5. After the computer-controlled approach had been completed, the parameters were changed to accommodate for scanning. Typical parameters included: bias = 5 V, set point = 0.4 nA, gain = 2 and time constant = 7. With the new parameters established, the STM was ready to begin scanning and searching for QDs.

All scanning and recording was done using the program **XMPPro™** by RHK Technology. Scanning often produced noisy or even useless results. Fortunately, several methods
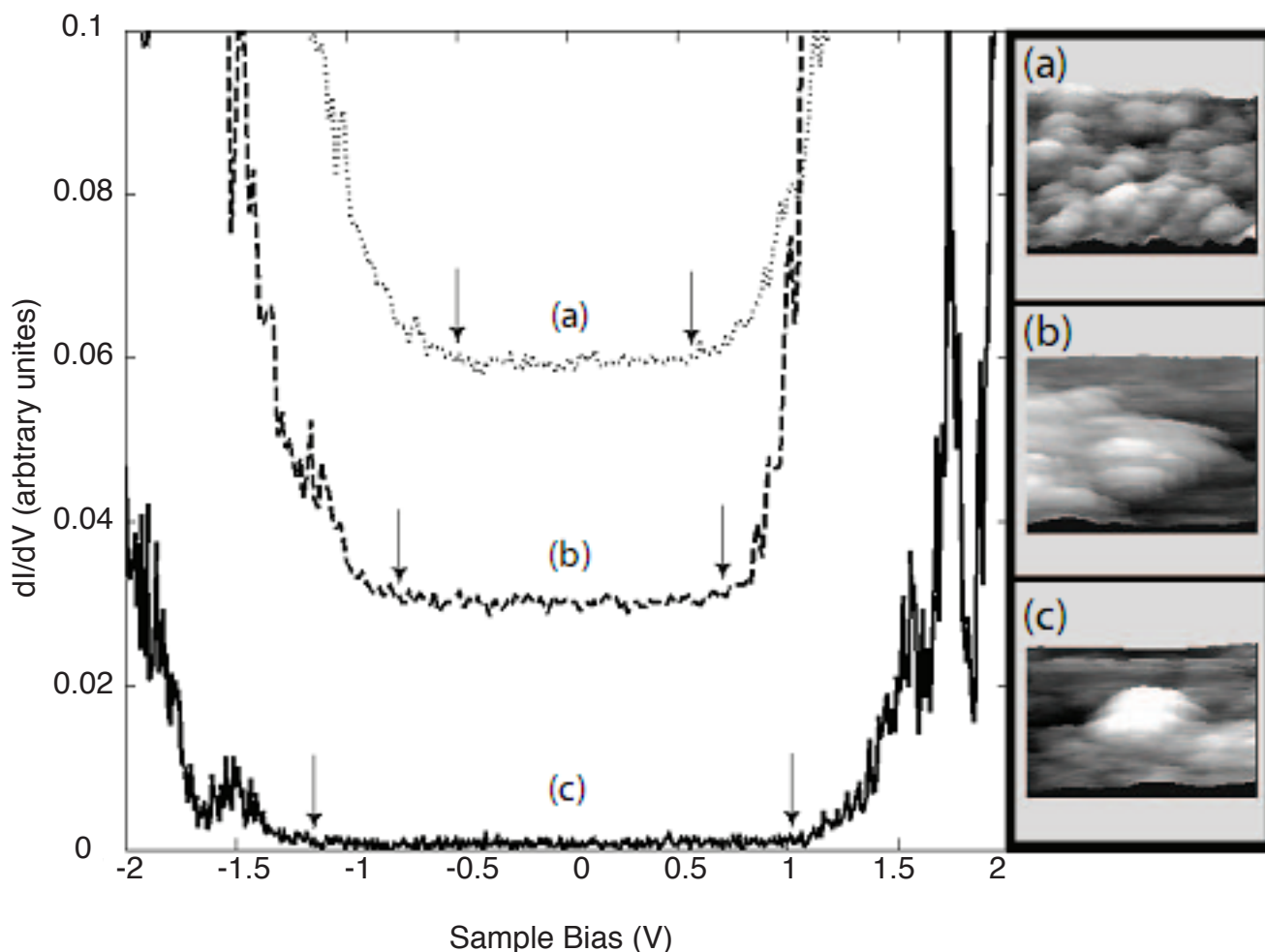

Figure 5. Spectra of differential conductance, dI/dV vs V, of colloidal CdSe quantum dots (d = 10 nm; optical bandgap 1.9 eV) on a Au substrate. The corresponding location of dots are (a) center of cluster (b) edge of cluster and (c) isolated. The bandgaps of the spectra are (a) 1.07 eV (b) 1.48 eV and (c) 2.18 eV. Spectra were obtained with It = 10 nA at a sample bias of Vt = 2:0 V.
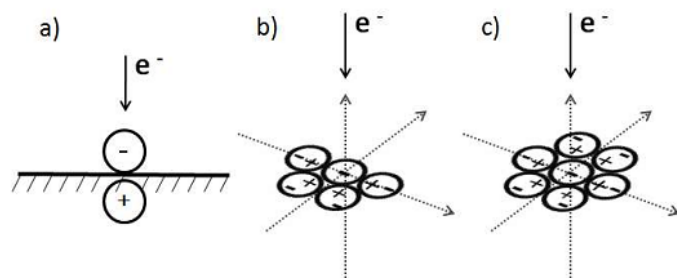
Figure 6. Schematics for the electrostatic screening models of: (a) isolated (horizontal line with hatches indicates Au surface) (b) edge of cluster and (c) center of cluster QDs. Circles mark dot locations with the exception of the positive charge in the gold surface and arrows indicate direction of tunneling current.

for reshaping the tip and producing better resolution have been found to work reasonably well. Alternating the bias between 1 V and 10 V could sometimes realign the particles in the tip into a better shape. The software also gave an option of two different pulses that acted on the bias in, essentially, the same way. Sometimes the problem was caused by a rough surface. In this case, simply relocating the image scan area could resolve the issue. Also, depending on the surface and/or background noise, the feedback loop may have been over or under reactive. To alleviate this problem, the gain, time constant and set point were adjusted accordingly. Eventually a clear image of dots would appear. Using the topographical image, the dots could be located by looking for surface bumps with a height around 10 nm. Once located, STS data was acquired on isolated, edge of cluster and center of cluster quantum dots.

Typically, when taking STS readings, the bias is set between 2.5 V and 3.5 V and the voltage sweep time is around 10 seconds per line. In this experiment the voltage range was placed from -2.0 V to +2.0 V. This range was chosen so that the region of zero-conductance could be seen easily if it were approximately the same as the observed optical bandgap. With the appropriate settings in place the tip could be located over a dot and the feedback loop could be turned off. The initial current was chosen by adjusting the tip height before the STS began. For comparison purposes, the current was kept at approximately 10 nA around 2 V.

Results

Spectroscopy measurements of conductance taken on 10 nm colloidal CdSe quantum dots in isolated and cluster environments (Figure 4) exhibited varying voltage ranges of zero-conductance. STS measurements of differential conductance (dI/dV) were simultaneously taken in order to evaluate the local density of states more closely. Typical images of QDs and their corresponding spectra taken at the location can be seen in Figure 5. The data was compiled

and analyzed in the MathWorks™ program MATLAB®. A dot in the center of a cluster (Figure 5a) had the smallest perceived bandgap (1.07 eV). A dot on the edge of a cluster (Figure 5b) had the slightly larger bandgap (1.48 eV). An isolated QD (Figure 5c) had the largest perceived bandgap (2.18 eV).

Discussion

Classical Electrostatics Model

Size-dependent effects on electronic spectra of nanocrystals have been rigorously explained and observed, but quantitative differences between theoretical calculations and experimental observations have been used to suggest that the model could be improved by incorporating Coulomb interactions.[3] It has been shown that since electrons are spatially confined to small volumes within quantum dots, the behavior of individual electrons has significant effects[2]; therefore, electrostatic forces are thought to play an important role.[4,5,9] For analytical purposes, each surface charge is treated as a point charge.

In the model, single electron charging or single hole charging occurs in the dot into which electrons are being tunneled, depending on the applied bias. In either case, the charge buildup acts to repel the direction of the tunneling current. To avoid unnecessary confusion, the model will be discussed in the case of a negative charge build-up on the dot with a positive bias on the sample, where electrons tunnel from the tip into the conduction band of the QD. As seen in Figure 6a, some of the repulsive force in the isolated dot model was countered by a positive image charge on the Au surface. In this set-up, a net Coulomb repulsion acted to widen the energy bandgap. Since CdSe nanocrystals are a polarizable material[8], the negative charge build up induced dipole moments on surrounding QDs. The induced dipole moments acted as a net positive charge around the tunneling dot and screened the negative charge on the QD being probed. Therefore, when neighboring QDs were introduced as in the edge of cluster model (Figure 6b), screening effects became significant enough to measure. With the addition of two more neighboring dots as exampled in the center of cluster model (Figure 6c), more dipoles were induced which enhanced the screening effect.

Graphical Analysis

The relative potentials of the three models in Figure 6 can be approximated using the potential formula

$$V(\vec{r}) = k \sum_{i=1}^{n} \frac{q_i}{r_i} \qquad (1)$$

where $k = \frac{1}{4\pi\epsilon_0}$ is the electrostatic constant, ϵ_0 is the permittivity of free space, q_i is the corresponding charge in electron volts and r_i is the distance from each charge to a test charge at the hypothetical location of the tip.

In this simplified model the dipoles are assumed to be single positive charges located at distance d = 10 nm away from the probed QD. The potential for each model in Figure 6 is solved for as a function of the tip to sample distance z giving

$$V_{iso}(z) = kq(\frac{1}{z+d} - \frac{1}{z}), \quad (2)$$

$$V_{edge}(z) = kq(\frac{1}{z+d} + \frac{5}{\sqrt{z^2+d^2}} - \frac{1}{z}), \quad (3)$$

and

$$V_{ctr}(z) = kq(\frac{1}{z+d} + \frac{7}{\sqrt{z^2+d^2}} - \frac{1}{z}) \quad (4)$$

for each type of environment (Figure 7). At a tip-to-dot distance of z = 1 nm, the relative repulsive energy V_r for each dot was calculated as a fraction of the net repulsive energy in the isolated case (V_0) giving a proportion of $0.45V_0$ for an edge dot and $0.23V_0$ for a dot in the center. The repulsive energy for each was used to roughly evaluate the measured or apparent bandgap

$$E_a = E_g - 2V_r \quad (5)$$

where E_g was the actual bandgap of the QD. Note that the repulsive energy was subtracted twice to account for repulsion in both the conduction and valence bands of the dot. Application of equation (5) demonstrated the dependency of the apparent bandgap on the number of neighboring dots.

Conclusion

It has been shown that an inverse relationship between the number of neighboring dots and the voltage range of zero-conductance exists. Having observed notable changes in the apparent bandgap, depending on the local environment of 10 nm CdSe nanocrystals, it concludes that an electrostatic screening model provided an overly simplified, but accurate, representation of the relationship. However, because of its overly simple nature, the model required much refinement. To improve the accuracy of this model, several other factors should be explored and addressed. Capacitance between the surface and dot caused by the ligand separation, and the variable capacitance between the tip and dot were two important issues neglected. The calculations of induced dipole moments should also account for the polarizability and the frequency dependence of the dielectric constant. Geometry of the surfaces was another important factor. Some questions arose in the interpretation of the location of each charge. When deciding on the value for z and d it was not clear if the charge build up on the dot should be treated as a point charge residing in the center of the dot, on
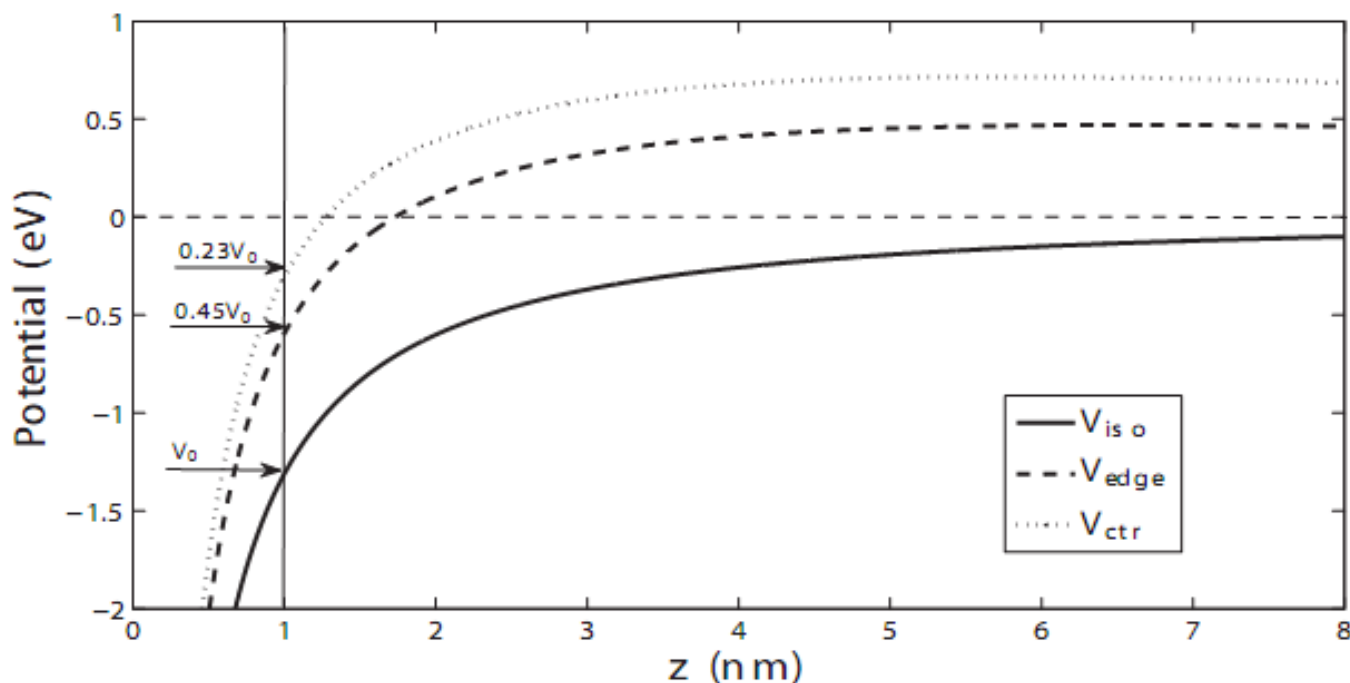

Figure 7. Graph of each function with the relative potentials labeled for each environment. Relative potentials were calculated using *d* = 10 nm and *z* = 1 nm. An accurate value of *V0* and the relative potential of each could be used to find the apparent bandgap.

the surface or as some charge density distribution. Determining the absolute tip-to-tip sample distance and varying the height with a set bias could provide more quantitative data needed to refine the model. Similarly, a study on the environmental effects of different materials and dot sizes would also be beneficial.

A thorough understanding of the electric properties of single and small clusters of QDs is very useful if they are to be applied to electronic devices. Using the knowledge of the electrostatic interactions between dot and surface and also dot and dot allows for more precise tuning of electrical and optical properties of the materials. These properties are essential if QDs are to be applied to quantum computation or solar cells.

Acknowledgements

References

[1] G. Binnig, H. Rohrer, C. Gerber, and E. Weibel, *Phys. Rev.* Lett. 49, 57 (1982).

[2] L. Candido, J. P. Rino, N. Studart, and F. M. Peeters, *Braz. J. Phys.* 27, 312 (1997).

[3] S. Coe, W. K. Woo, M. Bawendi, and V. Bulovic, *Nature* 420, 800 (2002).

[4] A. Franceschetti and M. C. Troparevsky, *Phys. Rev.* B 72, 165311 (2005).

[5] T. D. Krauss and L. E. Brus, *Phys. Rev.* Lett. 83, 4840 (1999).

[6] C. B. Murray, D. J. Norris, and M. G. Bawendi, J. *Am. Chem. Soc.* 115, 8706 (1993).

[7] D. J. Norris and M. G. Bawendi, *Phys. Rev.* B 53, 16338 (1996).

[8] A. J. Nozik, *Physica E* 14, 115 (2002).

[9] I. F. Torrente, K. J. Franke, and J. I. Pascual, J. Phys.; *Condens. Matter.* (UK) 20, 184001 (2008).

[10] A. Zrenner, M. Markmann, E. Beham, F. Findeis, G. Bohm, and G. Abstreiter, J. *Electron. Mater.* 28, 542 (1999).

SCIENCES